Pure Spin Current Injection in Hydrogenated Graphene Structures

Reinaldo Zapata-Peña[1], Bernardo S. Mendoza[1], Anatoli I. Shkrebtii[2]

[1]*Centro de Investigaciones en Óptica, León, Guanajuato 37150, México and*

[2]*University of Ontario, Institute of Technology, Oshawa, ON, L1H 7L7, Canada*

(Dated: April 21, 2017)

Lorem ipsum dolor sit amet, consectetuer adipiscing elit. Etiam lobortis facilisis sem. Nullam nec mi et neque pharetra sollicitudin. Praesent imperdiet mi nec ante. Donec ullamcorper, felis non sodales commodo, lectus velit ultrices augue, a dignissim nibh lectus placerat pede. Vivamus nunc nunc, molestie ut, ultricies vel, semper in, velit. Ut porttitor. Praesent in sapien. Lorem ipsum dolor sit amet, consectetuer adipiscing elit. Duis fringilla tristique neque. Sed interdum libero ut metus. Pellentesque placerat. Nam rutrum augue a leo. Morbi sed elit sit amet ante lobortis sollicitudin. Praesent blandit blandit mauris. Praesent lectus tellus, aliquet aliquam, luctus a, egestas a, turpis. Mauris lacinia lorem sit amet ipsum. Nunc quis urna dictum turpis accumsan semper.

I. INTRODUCTION

Lorem ipsum dolor sit amet, consectetuer adipiscing elit. Etiam lobortis facilisis sem. Nullam nec mi et neque pharetra sollicitudin. Praesent imperdiet mi nec ante. Donec ullamcorper, felis non sodales commodo, lectus velit ultrices augue, a dignissim nibh lectus placerat pede. Vivamus nunc nunc, molestie ut, ultricies vel, semper in, velit. Ut porttitor. Praesent in sapien. Lorem ipsum dolor sit amet, consectetuer adipiscing elit. Duis fringilla tristique neque. Sed interdum libero ut metus. Pellentesque placerat. Nam rutrum augue a leo. Morbi sed elit sit amet ante lobortis sollicitudin. Praesent blandit blandit mauris. Praesent lectus tellus, aliquet aliquam, luctus a, egestas a, turpis. Mauris lacinia lorem sit amet ipsum. Nunc quis urna dictum turpis accumsan semper. Lorem ipsum dolor sit amet, consectetuer adipiscing elit. Etiam lobortis facilisis sem. Nullam nec mi et neque pharetra sollicitudin. Praesent imperdiet mi nec ante. Donec ullamcorper, felis non sodales commodo, lectus velit ultrices augue, a dignissim nibh lectus placerat pede. Vivamus nunc nunc, molestie ut, ultricies vel, semper in, velit. Ut porttitor. Praesent in sapien. Lorem ipsum dolor sit amet, consectetuer adipiscing elit. Duis fringilla tristique neque. Sed interdum libero ut metus. Pellentesque placerat. Nam rutrum augue a leo. Morbi sed elit sit amet ante lobortis sollicitudin. Praesent blandit blandit mauris. Praesent lectus tellus, aliquet aliquam, luctus a, egestas a, turpis. Mauris lacinia lorem sit amet ipsum. Nunc quis urna dictum turpis accumsan semper.

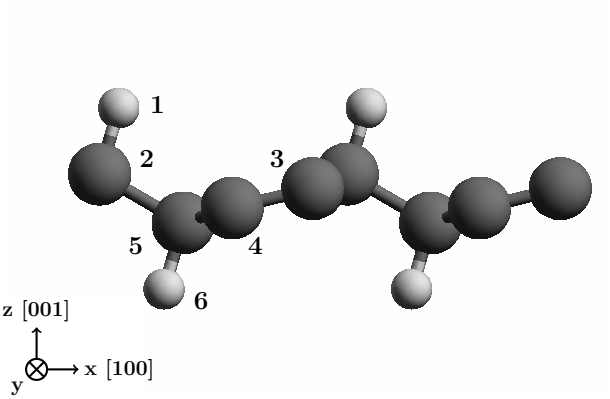

(a) xz plane view

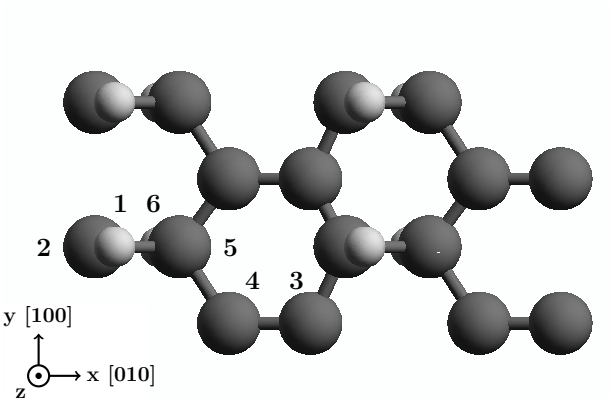

(b) xy plane view

FIG. 1. Alt structure.

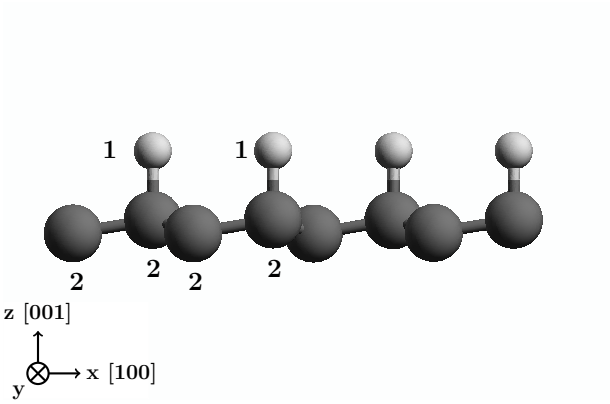

(a) xz plane view

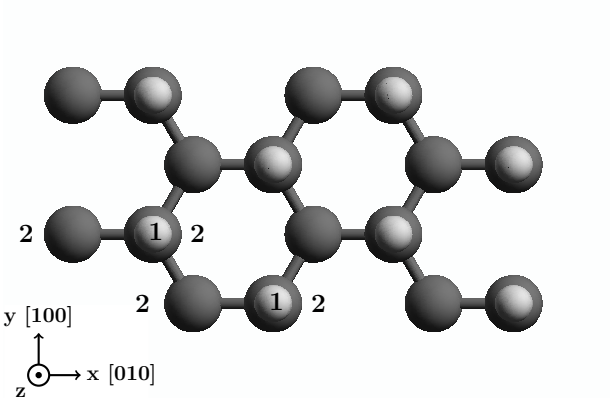

(b) xy plane view

FIG. 2. Up structure

Lorem ipsum dolor sit amet, consectetuer adipiscing elit. Etiam lobortis facilisis sem. Nullam nec mi et neque pharetra sollicitudin. Praesent imperdiet mi nec ante. Donec ullamcorper, felis non sodales commodo, lectus velit ultrices augue, a dignissim nibh lectus placerat pede. Vivamus nunc nunc, molestie ut, ultricies vel, semper in, velit. Ut porttitor. Praesent in sapien. Lorem ipsum dolor sit amet, consectetuer adipiscing elit. Duis fringilla tristique neque. Sed interdum libero ut metus. Pellentesque placerat. Nam rutrum augue a leo. Morbi sed elit sit amet ante lobortis sollicitudin. Praesent blandit blandit mauris. Praesent lectus tellus, aliquet aliquam, luctus a, egestas a, turpis. Mauris lacinia lorem sit amet ipsum. Nunc quis urna dictum turpis accumsan semper.

Lorem ipsum dolor sit amet, consectetuer adipiscing elit. Etiam lobortis facilisis sem. Nullam nec mi et neque pharetra sollicitudin. Praesent imperdiet mi nec ante. Donec ullamcorper, felis non sodales commodo, lectus velit ultrices augue, a dignissim nibh lectus placerat pede. Vivamus nunc nunc, molestie ut, ultricies vel, semper in, velit. Ut porttitor. Praesent in sapien. Lorem ipsum dolor sit amet, consectetuer adipiscing elit. Duis fringilla tristique neque. Sed interdum libero ut metus. Pellentesque placerat. Nam rutrum augue a leo. Morbi sed elit sit amet ante lobortis sollicitudin. Praesent blandit blandit mauris. Praesent lectus tellus, aliquet aliquam, luctus a, egestas a, turpis. Mauris lacinia lorem sit amet ipsum. Nunc quis urna dictum turpis accumsan semper.

II. THEORY

The equation for $\mathcal{V}^{\mathrm{ab}}$ for normal incidence in the xy plane with a polarization angle α is given by

$$\begin{aligned}\mathcal{V}^{\mathrm{ab}}(\omega) &= \frac{2}{\hbar}\frac{\mu^{\mathrm{abxx}}(\omega)E^2(\omega)\cos^2(\alpha)+\mu^{\mathrm{abyy}}(\omega)E^2(\omega)\sin^2(\alpha)+2\mu^{\mathrm{abxy}}(\omega)E^2(\omega)\cos(\alpha)\sin(\alpha)}{\xi^{\mathrm{xx}}(\omega)E^2(\omega)\cos^2(\alpha)+\xi^{\mathrm{yy}}(\omega)E^2(\omega)\sin^2(\alpha)},\\ &= \frac{2}{\hbar}\frac{\mu^{\mathrm{abxx}}(\omega)\cos^2(\alpha)+\mu^{\mathrm{abyy}}(\omega)\sin^2(\alpha)+\mu^{\mathrm{abxy}}(\omega)\sin(2\alpha)}{\xi^{\mathrm{xx}}(\omega)\cos^2(\alpha)+\xi^{\mathrm{yy}}(\omega)\sin^2(\alpha)}. \qquad (1)\end{aligned}$$

For an angle $\alpha = \frac{\pi}{4}$ this expression can be reduced to

$$\mathcal{V}^{\mathrm{ab}}(\omega) = \frac{2}{\hbar}\frac{\mu^{\mathrm{abxx}}(\omega)+\mu^{\mathrm{abyy}}(\omega)+2\mu^{\mathrm{abxy}}(\omega)}{\xi^{\mathrm{xx}}(\omega)+\xi^{\mathrm{yy}}(\omega)}. \qquad (2)$$

A. Fixing velocity.

Considering that we have 2D structures we fixed the velocity in the xy plane along x and y directions and we define $|\mathcal{V}^{\rm a}|$ as

$$|\mathcal{V}^{\rm a}| = \sqrt{(\mathcal{V}^{\rm ax})^2 + (\mathcal{V}^{\rm ay})^2 + (\mathcal{V}^{\rm az})^2}, \qquad (3)$$

and the corresponding polar and azimuthal angles θ and φ as

$$\theta = \cos^{-1}\left(\frac{\mathcal{V}^{\rm az}}{|\mathcal{V}^{\rm a}|}\right), \qquad 0 \leq \theta \leq \pi, \qquad (4)$$

$$\varphi = \tan^{-1}\left(\frac{\mathcal{V}^{\rm ay}}{\mathcal{V}^{\rm ax}}\right), \qquad 0 \leq \varphi \leq 2\pi. \qquad (5)$$

B. Fixing spin

In a similar way we can fix in the xy plane the spin direction along the x, y, and z directions and then define the magnitude of the spin velocity $|\mathcal{V}_{\sigma^{\rm b}}|$ in a fixed angle γ_b

$$|\mathcal{V}_{\sigma^{\rm b}}| = \sqrt{(\mathcal{V}^{\rm ax})^2 + (\mathcal{V}^{\rm ay})^2}, \qquad (6)$$

$$\gamma_{\rm b} = \tan^{-1}\left(\frac{\mathcal{V}^{\rm ay}}{\mathcal{V}^{\rm ax}}\right), \qquad (7)$$

where the angle is measured in the counterclockwise direction from the positive x axis.

III. RESULTS

We preset the results for $\mathcal{V}^{\rm ab}$ for the $C_{16}H_8$-alt and $C_{16}H_8$-up structures being both noncentrosymmetric semi-infinite carbon systems with 50% hydrogenation in different arrangements. The *alt* system has alternating hydrogen atoms on the upper and bottom sides of the carbon sheet, while the *up* system has H only on the upper side. We take the hexagonal carbon lattice to be on the xy plane for both structures, and the carbon-hydrogen bonds on the perpendicular xz plane, as depicted in Figs. 1 and 2.

Using the ABINIT code[1] we calculated the self- consistent ground state and the Kohn-Sham states using density functional theory in the local density approximation (DFT-LDA) with a planewave basis. We used Hartwigsen-Goedecker-Hutter (HGH) relativistic separable dual-space Gaussian pseudopotentials[2] including the spin-orbit interaction for calculating $\mathcal{V}^{\rm a}(\omega)$.

Layer No.	Atom type	Position [Å] x	y	z
1	H	-0.61516	-1.42140	1.47237
2	C	-0.61516	-1.73300	0.39631
3	C	0.61516	1.73300	0.15807
4	C	0.61516	0.42201	-0.15814
5	C	-0.61516	-0.37396	-0.39632
6	H	-0.61516	-0.68566	-1.47237

TABLE I. Unit cell of *alt* structure. Layer division, atom types and positions for the *alt* structure. The structure unit cell was divided in six layers corresponding each one to atoms in different z positions. The corresponding layer atom position is depicted in Fig. 1 with the corresponding number of layer.

The convergence parameters for the calculations of our results corresponding to the *alt* and *up* structures are cutoff energies of 65 Ha and 40 Ha, respectively. The energy eigenvalues and matrix elements were calculated using 14452 **k** points and 8452 **k** points in the irreducible Brillouin zone (IBZ) and present LDA energy band gaps of 0.72 eV and 0.088 eV, respectively for the *alt* and *up* structures. As mentioned in[3], using DFT the LDA is only one method of many other that can be used to calculate the electronic structure of materials. Also it is known that all methods predict a different band gap than the obtained in the experiment. A correction for the band gap energy value can be calculated by other *ab-initio* methods such as the GW approximation[4] being this outside the scope of this paper.

The structures presented here where divided into layers to analyze the he layer-by-layer contribution for $\mathcal{V}^{\rm ab}$ response. The *alt* structure was divided in six layers corresponding the first one to the top hydrogen atoms, from the second to the forth to carbon atoms in different z positions, and the sixth and last one to the bottom hydrogen atoms. The *up* structure was divided into two layers, the first one comprised by the top hydrogen atoms and the second by the carbon atoms. The layer divisions and atom positions for the unit cells are shown in Tables I and II.

Layer No.	Atom type	Position [Å] x	y	z
1	H	-0.61516	-1.77416	0.73196
1	H	0.61518	0.35514	0.73175
2	C	-0.61516	-1.77264	-0.49138
2	C	-0.61516	-0.35600	-0.72316
2	C	0.61516	0.35763	-0.49087

TABLE II. Unit cell of *up* structure. Layer division, atom types and positions for the *up* structure. The structure unit cell was divided in two layers corresponding to hydrogen and carbon atoms.The corresponding layer atom position is depicted in Fig. 2 with the corresponding number of layer.

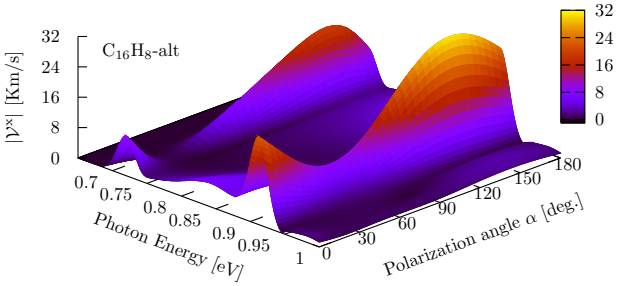

(a) $|\mathcal{V}^{x}|$ for *alt* structure

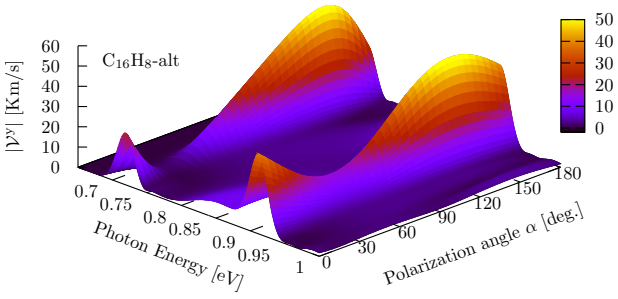

(b) $|\mathcal{V}^{x}|$ for *alt* structure

FIG. 3. $|\mathcal{V}^{x}|$ response for $C_{16}H_8$-alt structure. The maximum response zone is localized for an energy range from 0.90 eV to 0.93 eV. 145° and for a polarization angle of the incoming beam from 120° to 150°.

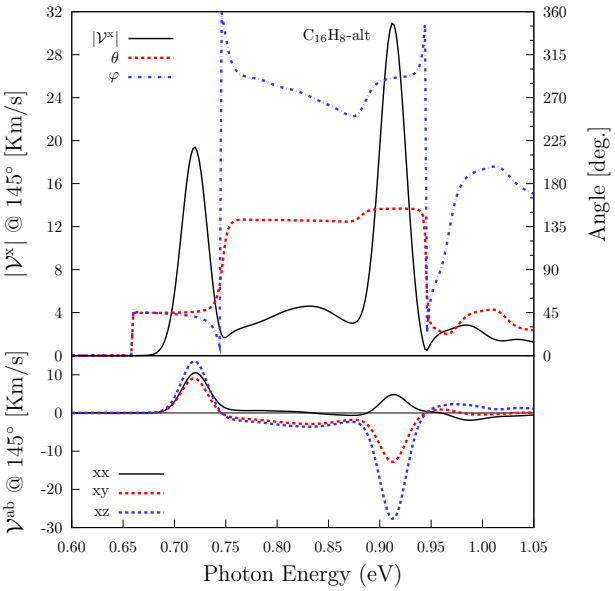

(a) $|\mathcal{V}^{x}|$

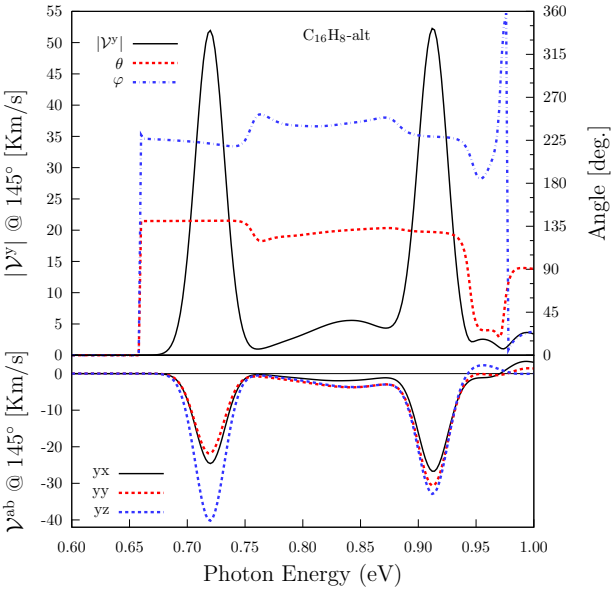

(b) $|\mathcal{V}^{x}|$

FIG. 4. Most intense responses of $|\mathcal{V}^{x}|$ and $|\mathcal{V}^{y}|$ and the corresponding three components for the *alt* structure. Both maxima where obtained for a polarization angle $\alpha = 145°$.

A. Fixing velocity

For the *alt* structure we analyzed the energy range of energy from 0.6 eV to 1.0 eV where we found the most intense response for $\mathcal{V}^{ab}$ and $|\mathcal{V}^{a}|$. In Fig. 3 we present the $|\mathcal{V}^{a}|$ spectra resulting from evaluate Eq. (3) using different polarization angles α in Eq. (1) for the $C_{16}H_8$-alt structure. We can see that the onset of the response is when the energy of the incoming light is the same of the gap energy. From this picture we can see that for the zone between the energy range of 0.90 eV-0.93 eV and polarization angles between 120° and 150° is the zone of the ab-

solute maximum response having for both, $|\mathcal{V}^{x}|$ and $|\mathcal{V}^{y}|$. Also there is another zone of interest for energies from 0.70 eV to 0.74 eV where a local maximum is obtained. From Fig. III A we have that $|\mathcal{V}^{x}|$reaches values near to 30 Km/s for the first zone mentioned before and 20 Km/s for the second one. We also found that the absolute maximum of the response is obtained for a polarization angle $\alpha = 145°$. The decomposition of $|\mathcal{V}^{x}|$ in the corresponding $\mathcal{V}^{xx}$, $\mathcal{V}^{xy}$, and $\mathcal{V}^{xz}$ components is depicted in Fig. III A and the decomposition of $|\mathcal{V}^{y}|$ in its corresponding $\mathcal{V}^{yx}$, $\mathcal{V}^{yy}$, and $\mathcal{V}^{yz}$ is shown in Fig. III A for this polarization angle. Making the analysis for $|\mathcal{V}^{x}|$ we can see that for the energy range from 0.70 eV to 0.74 eV all the xx, xy, and xz components contribute with almost the same intensity giving a total spin-velocity near to 30 Km/s. In the other hand, for the energy range from 0.88 eV to 0.95 eV there is a major contribution coming from the $\mathcal{V}^{xz}$ component resulting in a spin-velocity near to 20 Km/s. Also we notice that for the range of 0.70-0.74 eV all the contributions are positive while for the range of 0.88-0.95 eV the xx component remains positive but the components xy and xz change in direction. This is due to a change in the spin polarization. Making now the analysis for $|\mathcal{V}^{y}|$, which is almost two times more intense than $|\mathcal{V}^{x}|$, we have that for the energy range from 0.70 eV to 0.74 eV the yx and yy components have a lesser contribution than yz but for the energy range all three components have almost the same intensity resulting in a spin-velocity near to 50 Km/s in both cases. Now we have that the three components of $|\mathcal{V}^{y}|$ are negative for the energy range from 0.65 eV to 0.95 eV keeping the same spin polarization for all this range.

[1] X. Gonze, B. Amadon, P.-M. Anglade, J.-M. Beuken, F. Bottin, P. Boulanger, F. Bruneval, D. Caliste, R. Caracas, M. Côté, T. Deutsch, L. Genovese, P. Ghosez, M. Giantomassi, S. Goedecker, D. Hamann, P. Hermet, F. Jollet, G. Jomard, S. Leroux, M. Mancini, S. Mazevet, M. Oliveira, G. Onida, Y. Pouillon, T. Rangel, G.-M. Rignanese, D. Sangalli, R. Shaltaf, M. Torrent, M. Verstraete, G. Zerah, and J. Zwanziger, Comput. Phys. Commun. **180**, 2582 (2009).

[2] C. Hartwigsen, S. Goedecker, and J. Hutter, Phys. Rev. B **58**, 3641 (1998).

[3] R. Zapata-Peña, S. M. Anderson, B. S. Mendoza, and A. I. Shkrebtii, physica status solidi (b) **253**, 226 (2016).

[4] G. Onida, L. Reining, and A. Rubio, Rev. Mod. Phys. **74**, 601 (2002).